

# Hilbert Transform on Graphs: Let There Be Phase

Michael Chan, *Student Member, IEEE*, Alexandre Cionca, *Student Member, IEEE*,  
Dimitri Van De Ville, *Fellow, IEEE*

**Abstract**—In the past years, many signal processing operations have been successfully adapted to the graph setting. One elegant and effective approach is to exploit the eigendecomposition of a graph shift operator (GSO), such as the adjacency or Laplacian operator, to define a graph Fourier transform when projecting graph signals on the corresponding basis. However, the extension of this scheme to directed graphs is challenging since the associated GSO is non-symmetric and, in general, not diagonalizable. Here, we build upon a recent framework that adds a minimal number of edges to allow diagonalization of the GSO and thus provide a proper graph Fourier transform. We then propose a generalization of the Hilbert transform that leads to a number of simple and elegant recipes to effectively exploit the phase information of graph signals provided by the graph Fourier transform. The feasibility of the approach is demonstrated on several examples.

**Index Terms**—Graph signal processing, Harmonic analysis, Hilbert transform, Directed graph.

## I. INTRODUCTION

GRAPH signal processing (GSP) has emerged as an attractive new methodology for analyzing structured data [1]–[3]. In most cases, an undirected graph is considered, which implies a symmetric adjacency matrix. The definition of the graph Fourier transform (GFT) by the eigendecomposition of a graph shift operator (GSO) [4], typically the adjacency or Laplacian matrix, leads then to real-valued eigenvalues and eigenvectors, and constitutes an unitary transform for the analysis and synthesis of graph signals. Different operations, such as filtering, can then be defined and implemented in the spectral graph domain [5]–[7].

For directed graphs, however, the GSO becomes non-symmetric and is in general non-diagonalizable. The Jordan normal form (JNF) has been suggested for providing the spectral decomposition of the GSO [8]. However, this comes with several complications. First, the JNF is numerically unstable [9], especially for larger graphs. Second, non-trivial Jordan blocks correspond to spectral components with dimension larger than one, which impede GSP operations such as filtering and sampling [10].

Following these two main problems in the numerical application of the JNF in GSP, alternatives have been developed to ensure orthogonality through optimized bases [11], [12]. Both these works introduce directed total variation measures and yield real bases. Moreover, [12] finds bases with uniformly

sampled frequency. However, both methods only work on real signals and bypass the GSO, meaning that only spectrum-based operations would be allowed. Another approach proposed is to once again bypass the standard GSO and instead use the diagonalizable Hermitian Laplacian [13], which leads to a basis that fulfils Parseval property. These alternatives would fulfill properties such as orthogonality, evenly spread frequencies, and most importantly diagonalizability, but turn out to largely alter the underlying graph structure.

In this work, we start from the perspective to consider the Graph Fourier Transform (GFT) on directed graph through projection on a basis derived from the adjacency matrix as GSO [4]. Secondly, we leverage recent work [14] that proposed to destroy non-trivial Jordan blocks by adding a minimal amount of edges to the directed graph. This method enables conventional diagonalization of the modified graph adjacency, and thus permits to define the GFT as the projection on the dual basis derived from the GSO eigendecomposition. Intuitively, the addition of edges creates cyclicity in subgraphs necessary to reduce Jordan Blocks to dimensionality 1, thus enabling diagonalization. Furthermore, such edges could also be added to remove Jordan Blocks associated to eigenvalues 0, thus allowing for invertibility. This method also proves [14] to yield a minimally different (spectrally) approximation of the original adjacency. The newly generated adjacency remain a real-valued matrix that brings an eigendecomposition with eigenvalues that are either real-valued or pairs of complex conjugates [15]. Thus a parallel can be drawn between traditional Discrete Fourier Transform’s (DFT) pairs of conjugate frequencies and the pairs of conjugate eigenvalues found in the presented eigendecomposition of the diagonalizable directed graph. A direct application of this property is the Hilbert Transform. Prior work defining the Graph Hilbert Transform (GHT) [15] shows its equivalence to the traditional Hilbert Transform while not giving a practical method to apply GHT since they assume both diagonalizability and invertibility. Instead, here we propose the use of the mentioned minimal graph perturbation to render the GSO diagonalizable and invertible. Then we introduce a more straightforward definition of the GHT providing interpretation for instantaneous phase and amplitude. We further highlight its properties and specifically the extension to the graph analytical signal by insightful examples.

## II. FROM GRAPH PHASE TO HILBERT TRANSFORM

In what follows, we denote a matrix  $\mathbf{X}$  as bold uppercase and a vector  $\mathbf{x}$  as bold lowercase. An element  $k$  of a vector will be indicated as  $\mathbf{x}[k]$  and a series of vectors  $\mathbf{x}_m$  will be indexed using subscript. The conjugate will be written as  $\cdot^*$ .

M. Chan, A. Cionca and D. Van De Ville are with the Neuro-X Institute, Ecole polytechnique fédérale de Lausanne, and the Department of Radiology and Medical Informatics, University of Geneva, Switzerland. E-mail: chunheimichael.chan@epfl.ch

This work was supported in part by the Swiss National Science Foundation, Sinergia project “Precision mapping of electrical brain network dynamics with application to epilepsy”, Grant number 209470.

Manuscript received XXX; revised XXX.

### A. Phase in the Graph Fourier Domain

Let us consider a directed graph  $\mathcal{G} = (V, E)$ , with  $V$  being the set of nodes and  $E$  the set of edges. The directed graph  $\mathcal{G}$  has  $N$  nodes and is also characterized by the (non-symmetric) adjacency matrix  $\mathbf{A}$ . The perturbed adjacency  $\mathbf{A}'$  according to [14] is guaranteed to be diagonalizable and invertible. Thus we consider the eigendecomposition of the perturbed adjacency:

$$\mathbf{A}' = \mathbf{U}\mathbf{\Lambda}\mathbf{U}^{-1},$$

where the eigenvalues  $\Lambda[k, k] = \lambda_k$  are either real-valued with corresponding real-valued eigenvectors  $\mathbf{u}_k, k = 1, \dots, N$ , that are the columns of  $\mathbf{U}$ ; or complex-valued, and then come in pairs of complex conjugate eigenvalues and eigenvectors, for instance, for a pair a complex-valued eigenvalues with indexes  $(k_1, k_2)$ , we have  $\lambda_{k_1} = \lambda_{k_2}^*$  with eigenvectors  $\mathbf{u}_{k_1} = \mathbf{u}_{k_2}^*$ . Therefore, the GFT  $\hat{\mathbf{x}} = \mathbf{U}^{-1}\mathbf{x}$  of a real-valued graph signal  $\mathbf{x} \in \mathbb{R}^N$  will also have complex conjugate coefficients for these pairs; i.e.,  $\hat{\mathbf{x}}[k_1] = \hat{\mathbf{x}}[k_2]^*$ .

### B. Graph Hilbert Transform and Analytical Graph Signal

We introduce the GHT by defining the following filter in the spectral domain by the diagonal matrix  $\hat{\mathbf{H}}$ :

$$\hat{\mathbf{H}}[k, k] = \begin{cases} -j, & \text{imag}(\lambda_k) > 0, \\ +j, & \text{imag}(\lambda_k) < 0, \\ 0, & \text{imag}(\lambda_k) = 0. \end{cases} \quad (1)$$

GFT coefficients corresponding to complex-valued adjacency eigenvalues are multiplied with  $-j$  and  $+j$  according to the sign of the imaginary part of the eigenvalues, respectively. A positive/negative imaginary part of the eigenvalue can be interpreted as a positive/negative frequency. As mentioned before, GFT coefficients of a real-valued graph signal are complex conjugate for the pairs of complex eigenvalues. Therefore, the Hilbert transform  $\mathcal{H}(\mathbf{x}) = \mathbf{U}\hat{\mathbf{H}}\mathbf{U}^{-1}\mathbf{x}$  of such a graph signal is also real-valued. Furthermore, spectral filtering by  $\hat{\mathbf{H}}$  possesses properties of linearity and commutativity with polynomials of the GSO. Subsequently, we can define the analytical graph signal as

$$\mathbf{x}_a = \mathbf{x} + j\mathcal{H}(\mathbf{x}) = \mathbf{U}(\mathbf{I} + j\hat{\mathbf{H}})\hat{\mathbf{x}}, \quad (2)$$

which can be represented in terms of instantaneous amplitudes and phases:

$$\begin{aligned} \mathcal{A}(\mathbf{x})[k] &= \|\mathbf{x}_a[k]\|, \\ \varphi(\mathbf{x})[k] &= \arctan(\text{Im}(\mathbf{x}_a[k]), \text{Re}(\mathbf{x}_a[k])). \end{aligned}$$

### C. Interpretation of Graph Hilbert Transform

In traditional signal processing, the instantaneous amplitude and phase of the Hilbert transform is given the interpretation of the magnitude of the signal envelop and the phase within the underlying oscillatory pattern, respectively. This interpretation still applies for a directed cycle graph, which is a model for a 1-D discrete signal with periodic boundary conditions. For a more general graph, we need to acknowledge its structure in terms of subcycles. The method that destroys non-trivial Jordan blocks allows us to infer the existence of these subcycles, where each fulfills periodic boundary conditions. With the

following proposition, we provide a generalized interpretation to the GHT instantaneous amplitude and phase.

**Proposition 1.** *If the graph  $\mathcal{G}$  is minimally perturbed following [14] and thus allows diagonalization and invertibility of its corresponding adjacency matrix  $\mathbf{A}$ , then  $\mathcal{G}$  can be decomposed into  $M$  spanning subcycles  $\mathcal{C}_1, \mathcal{C}_2, \mathcal{C}_3, \dots, \mathcal{C}_M$ . Given a graph signal  $\mathbf{x}_i \in \mathbb{R}^N$  supported on a subcycle  $\mathcal{C}_m$  (i.e.,  $\mathbf{x}_m[k] = 0$  for  $k \notin \mathcal{C}_m$ ), then the following properties of the Hilbert amplitude and phase of the graph signal  $\mathbf{x} = \sum_{m=1}^M \mathbf{x}_m$  hold:*

$$\begin{aligned} \mathcal{A}(\mathbf{x})[k]^2 &= \sum_{m=1}^M \mathcal{A}(\mathbf{x}_m)[k]^2 \\ &+ \sum_{m \neq n}^M \mathbf{x}_m[k]\mathbf{x}_n[k] + \mathcal{H}(\mathbf{x}_m)[k]\mathcal{H}(\mathbf{x}_n)[k], \\ \varphi(\mathbf{x})[k] &= \arctan\left(\sum_{m=1}^M \mathcal{H}(\mathbf{x}_m)[k], \sum_{m=1}^M \mathbf{x}_m[k]\right). \end{aligned}$$

*Proof.* First, let us show that the graph  $\mathcal{G} = (V, E)$  after the modification of [14] admits a cycle cover, in other words that  $\mathcal{G}$  is 0-acyclic. For this purpose, we follow [16] and consider the space  $S_{\mathcal{G}}$ , set of matrices associated to subgraphs of  $\mathcal{G}$  such that  $\mathcal{G}_{sub} = (V, E_{sub})$  and  $E_{sub} \subseteq E$ . A graph is  $r$ -acyclic if and only if every matrix  $A_{sub} \in S_{\mathcal{G}}$  has at least  $r$  zero eigenvalues [16, Th. 4.4]. By contradiction let us assume that our graph  $\mathcal{G}$  is  $r$ -acyclic with  $r \neq 0$ . However, the associated adjacency matrix  $A \in S_{\mathcal{G}}$  has no zero eigenvalues due to the construction of [14]. Therefore, there exists a matrix belonging to  $S_{\mathcal{G}}$  with no zero eigenvalues, which leads to a contradiction, and, therefore,  $\mathcal{G}$  can only be 0-acyclic, meaning that  $\mathcal{G}$  can be decomposed into  $M$  spanning subcycles  $\mathcal{C}_1, \mathcal{C}_2, \mathcal{C}_3, \dots, \mathcal{C}_M$ .

Second, consider graph signals  $\mathbf{x}_m \in \mathbb{R}^N$  associated to the subcycles  $\mathcal{C}_m$  such that  $\mathbf{x}_m[k] = 0$  for  $k \notin \mathcal{C}_m$ . Then the following derivation is valid for the graph signal  $\mathbf{x} = \sum_{m=1}^M \mathbf{x}_m$ :

$$\begin{aligned} \mathcal{A}(\mathbf{x})[k]^2 &= \left\| \sum_{m=1}^M \mathbf{x}_m[k] + j\mathcal{H}(\mathbf{x}_m)[k] \right\|^2 \\ &= \left( \sum_{m=1}^M \mathbf{x}_m[k] \right)^2 + \left( \sum_{m=1}^M \mathcal{H}(\mathbf{x}_m)[k] \right)^2 \\ &= \sum_{m=1}^M \mathcal{A}(\mathbf{x}_m)[k]^2 \\ &+ \sum_{m \neq n}^M \mathbf{x}_m[k]\mathbf{x}_n[k] + \mathcal{H}(\mathbf{x}_m)[k]\mathcal{H}(\mathbf{x}_n)[k]. \end{aligned}$$

The phase  $\varphi(\mathbf{x})[k]$  similarly follows from the definition and linearity of the Hilbert transform:

$$\varphi(\mathbf{x})[k] = \arctan\left(\sum_{m=1}^M \mathcal{H}(\mathbf{x}_m)[k], \sum_{m=1}^M \mathbf{x}_m[k]\right).$$

□

These properties explain how the signals from different cycles combine for overlapping nodes i.e nodes of overlapping subcycles. For a node  $k$  that exclusively belongs to one subcycle  $\mathcal{C}_m$ , we have  $\mathbf{x}[k] = \mathbf{x}_m[k]$  and thus the equations revert

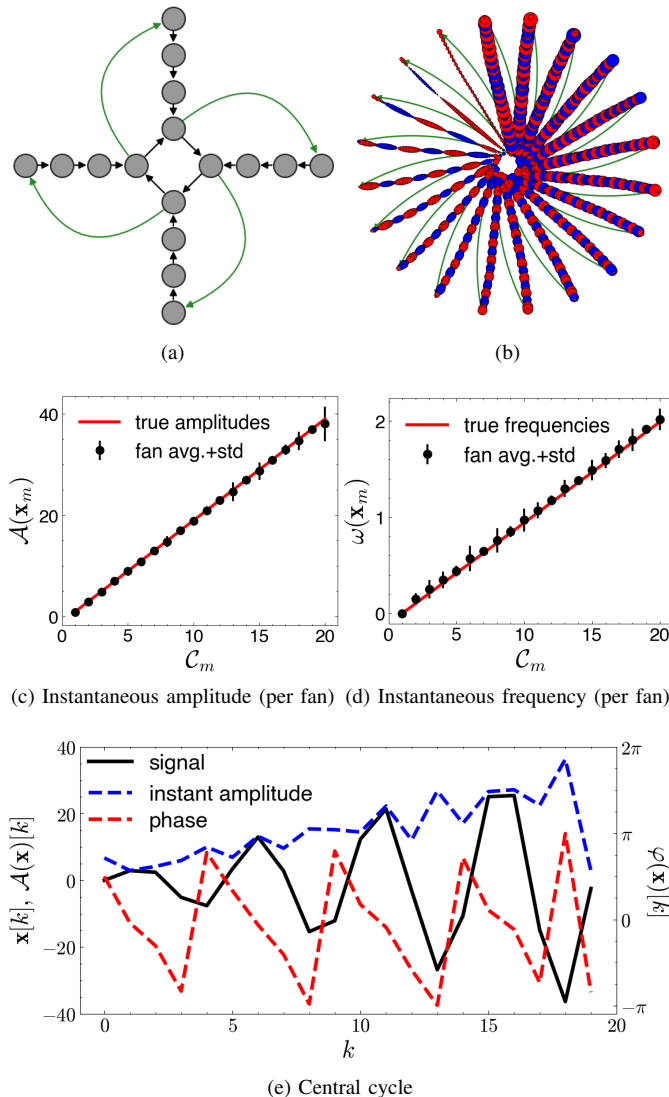


Fig. 1. (a) Schematic of synthetic graph. The green edges indicates those that are added to render the graph's adjacency matrix diagonalizable and invertible. (b) Synthetic graph and graph signal. The green edges are again the ones of the modified graph. (c) Instantaneous amplitude distribution across fans  $C_m$ . (d) Instantaneous frequencies distribution across fans  $C_m$ . (e) Graph signal, instantaneous amplitude and phase on the central cycle.

to the conventional interpretation of instantaneous amplitude and phase in that cycle. For nodes of overlapping subcycles, the degree of mixing will depend on the relevant strengths of the contributing signals  $\mathbf{x}_m$ . Notice that the decomposition of  $\mathbf{x}$  into a set of  $\mathbf{x}_m$  is not unique, although all possible decompositions will combine into the same apparent instantaneous amplitude and phase of  $\mathbf{x}$ .

### III. EXPERIMENTAL RESULTS

#### A. Setup

To illustrate and better understand the GHT in terms of instantaneous amplitude and phase on graphs, we provide a number of test cases.

1) *Synthetic Data*: The structure of our first graph is illustrated in Fig. 1a and consists of a central directed cycle graph

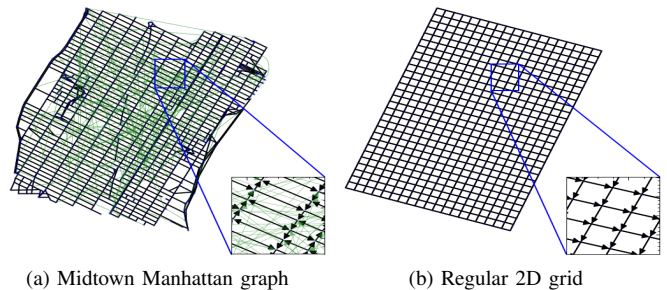


Fig. 2. (a) The midtown Manhattan street plan is providing the basis for this directed graph. In green, edges of the modified graph are indicated. (b) The regular 2D grid is composed of horizontal edges going from left to right and vertical edges going from top to bottom, additionally each verticals and horizontals are cycles.

with  $N_C$  nodes that each have an outgoing fan containing  $N_F$  nodes, including the starting node from the central cycle. Therefore, the total number of nodes is  $N_C N_F$ . We associate to each outgoing fan a sinusoidal signal of varying frequency and amplitude according to the following equation:

$$\mathbf{x}_m[k] = (2m + 1) \sin \left( \frac{m + 1}{N_f} 2\pi k + \frac{N_c + 1}{5N_c} 2\pi m \right),$$

which creates sinusoidal signals with increasing frequency and amplitude on the fans, and at the same time a signal with fixed frequency on the central cycle.

2) *Experimental Data*: From the Manhattan graph [17], we take the midtown subgraph composed of many one-way avenues and streets (in both directions), see Fig. 2a. We also created a graph from a regular 2D grid of similar size where the nodes are connected from top-to-bottom and left-to-right with periodic boundary conditions, see Fig. 2b. As a graph signal, we created a planar wave pattern along the direction of the avenues (i.e., approximately north-south). The frequency of the wave is chosen such that one period covers the midtown area. The graph signal is illustrated in Fig. 3a, 3c on respectively the regular 2D grid and midtown Manhattan graph.

#### B. Results

1) *Synthetic Data*: We instantiate the graph of Fig. 1a for  $N_C = 20$  fans of length  $N_F = 60$ . The adjacency matrix is neither diagonalizable nor invertible, with the Jordan block decomposition providing  $N_C$  blocks with eigenvalues zero. Destroying the non-trivial Jordan blocks leads to the directed rosace graph as shown schematically in Fig. 1b, turning fans into subcycles linked to the central part. When analyzing the graph signal using the GHT, we computed the instantaneous amplitude and phase for all nodes. Then, the instantaneous phase was converted into instantaneous frequency by computing the phase-unwrapped derivative along the fan as follows

$$\omega(\mathbf{x})[k] = (\varphi(\mathbf{x})[k] - \varphi(\mathbf{x})[k_{+1}]) + 2l\pi, \quad (3)$$

where  $k_{+1}$  indicates the next node on the fan and  $l$  is the integer that turns  $\omega$  in the interval  $]-\pi, \pi]$  following Itoh's unwrapping method [18]. As shown in Figs. 1c and 1d, the

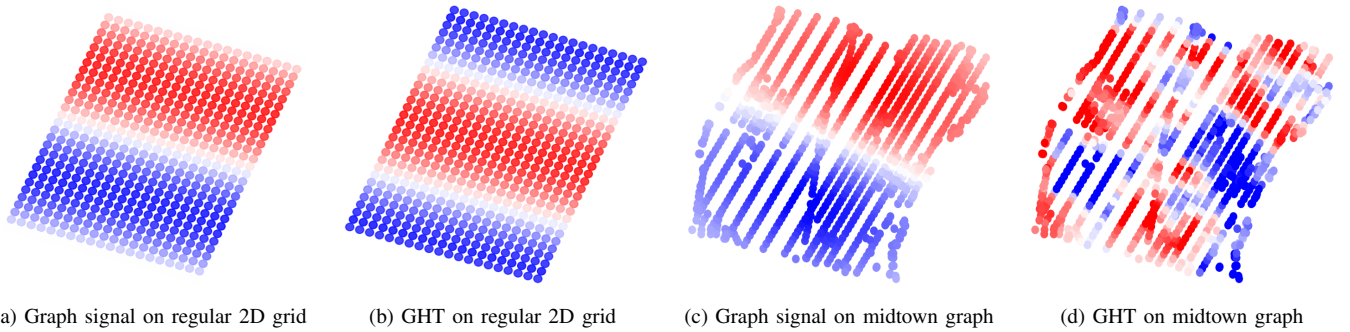


Fig. 3. (a) Graph signal is a planar wave oriented along the same direction as avenues in Fig. 3c. (b) On the regular 2D grid, the GHT of the graph signal shows a clear  $\pi/2$  phase shift along propagation direction. (c) Graph signal is a planar wave oriented along the avenues. (d) On the Manhattan midtown graph, the GHT of the graph signal reveals the effect of the underlying directed graph in phase shifting.

average amplitude and frequency per fan are accurate estimates of the ground truth expressed in the synthetic graph signal. In addition, the instantaneous amplitude and phase on the central cycle is also in accordance with our expectation of what the Hilbert transform should do; i.e., the amplitude recovers the envelope of the oscillating and increasing signal, and the phase varies constantly since the frequency is fixed on the central cycle.

This example perfectly illustrates Proposition 1. First, the GHT is fully in line with the classical Hilbert transform on the fans that form non-overlapping cycles, and thus amplitude, phase, and frequency are perfectly recovered. Second, the GHT has the capability to provide similar properties for an overlapping cycle (i.e., the central cycle of this graph). It is clear that the graph signal expressed on the central cycle is “compatible” with the one on the fans. Nevertheless, instantaneous amplitude and phase are in accordance with the meaning of the conventional Hilbert transform.

2) *Experimental Data:* The adjustment of the adjacency matrix of the Manhattan midtown graph leads to 252 extra edges (compared to the 1970 original ones) that are indicated in green in Fig. 2a. The graph based on the regular 2D grid does not require any adjustment. First, we look at the effect of the GHT on the planar wave graph signal expressed on the regular grid. We observe a phase shift of  $\pi/2$  along the propagation direction, turn turning the sine into a cosine, as illustrated in Fig. 3b. Second, as shown in Fig. 3d, the GHT of the same signal expressed on the Manhattan midtown graph produces a complicated scattering of wave due to the intricate pattern of directed edges (by one-way streets and avenues crossing, see Fig. 2a). We can recognize different patterns in the east and west of the midtown.

### C. Implementation

Documented code is openly available on the following GitHub repository<sup>1</sup>. The implementation is provided in Python and integrates the graph diagonalization and invertibilization algorithm along with additional features. A reproducible notebook of the study case shown in our paper is featured with a stable implementation of GHT.

<sup>1</sup><https://github.com/miki998/Graph-Hilbert-Transform>

## IV. DISCUSSION & OUTLOOK

While the Hilbert transform has been extended previously to the directed graph setting [15] in a similar way, we highlight here that it is key for the eigendecomposition of the GSO to be well-defined; i.e., diagonalizable and invertible. We rely on the scheme of [14] that destroys non-trivial Jordan blocks of the GSO and thus ensures its proper eigendecomposition. In addition, we provide an interpretation of the GHT in terms of the decomposition of the graph signal in subcycles. Such a representation is not unique, nevertheless it provides a useful intuition on how the GHT combines information from different cycles. Our first example illustrates how the GHT matches the conventional Hilbert transform on non-overlapping cycles, and can remain interpretable on overlapping ones.

For a more general graph such as the Manhattan midtown graph, all nodes are overlapping nodes and directionality is complex. Interestingly, on a graph that corresponds to a regular 2-D grid, the GHT behaves as one would expect from monogenic signal analysis [19], [20]; i.e., the phase shift of the Hilbert transform occurs along the propagation direction of the planar wave. However, when applying the GHT on the midtown graph, the complexity of the graph structure is reflected in an intricate pattern that is phase-shifted differently in different parts. Notice that from the analytical graph signal, one can easily obtain the result of any amount of phase shifting as with the conventional Hilbert Transform.

In this work, we used the adjacency matrix as the GSO to ensure applicability in general graph and in particular ensured the invertibility of the adjacency matrix’s eigenvectors matrix. However using the directed Laplacian [21] as a GSO for GHT is also valid under the condition that its eigenvector matrix is invertible. Indeed, the definition of the GHT on conjugate pairs would remain sound thanks to the directed Laplacian having only real entries.

Future work can focus on applications where analysis of signals on a complex and irregular domain characterized by a directed graph, can benefit from the flexibility of the GHT. This paper also renews interest in the study of phase properties enabled by directed graphs, opening avenues for subsequent studies aimed at leveraging graph phase.

## REFERENCES

- [1] D. I. Shuman, S. K. Narang, P. Frossard, A. Ortega, and P. Vandergheynst, "The Emerging Field of Signal Processing on Graphs: Extending High-Dimensional Data Analysis to Networks and Other Irregular Domains," *IEEE Signal Processing Magazine*, vol. 30, pp. 83–98, May 2013. arXiv:1211.0053 [cs].
- [2] A. Ortega, P. Frossard, J. Kovačević, J. M. F. Moura, and P. Vandergheynst, "Graph Signal Processing: Overview, Challenges, and Applications," *Proceedings of the IEEE*, vol. 106, pp. 808–828, May 2018.
- [3] A. G. Marques, S. Segarra, and G. Mateos, "Signal Processing on Directed Graphs: The Role of Edge Directionality When Processing and Learning From Network Data," *IEEE Signal Processing Magazine*, vol. 37, pp. 99–116, Nov. 2020.
- [4] A. Sandryhaila and J. M. F. Moura, "Discrete Signal Processing on Graphs," *IEEE Transactions on Signal Processing*, vol. 61, pp. 1644–1656, Apr. 2013. arXiv:1210.4752 [physics].
- [5] A. Sandryhaila and J. M. Moura, "Big Data Analysis with Signal Processing on Graphs: Representation and processing of massive data sets with irregular structure," *IEEE Signal Processing Magazine*, vol. 31, pp. 80–90, Sept. 2014.
- [6] S. Chen, A. Sandryhaila, J. M. F. Moura, and J. Kovacevic, "Signal denoising on graphs via graph filtering," in *2014 IEEE Global Conference on Signal and Information Processing (GlobalSIP)*, (Atlanta, GA, USA), pp. 872–876, IEEE, Dec. 2014.
- [7] Xuesong Shi, Hui Feng, Muyuan Zhai, Tao Yang, and Bo Hu, "Infinite Impulse Response Graph Filters in Wireless Sensor Networks," *IEEE Signal Processing Letters*, vol. 22, pp. 1113–1117, Aug. 2015.
- [8] A. Sandryhaila and J. M. F. Moura, "Discrete Signal Processing on Graphs: Frequency Analysis," *IEEE Transactions on Signal Processing*, vol. 62, pp. 3042–3054, June 2014.
- [9] T. Beelen and P. V. Dooren, "Computational aspects of the Jordan canonical form," in *Reliable Numerical Computation* (M. G. Cox and S. Hammarling, eds.), pp. 57–72, Oxford University PressOxford, Sept. 1990.
- [10] J. Shi and J. M. F. Moura, "Graph Signal Processing: Modulation, Convolution, and Sampling," Dec. 2019. arXiv:1912.06762 [eess].
- [11] S. Sardellitti, S. Barbarossa, and P. Di Lorenzo, "Graph Fourier Transform for directed graphs based on Lovász extension of min-cut," in *2017 IEEE International Conference on Acoustics, Speech and Signal Processing (ICASSP)*, (New Orleans, LA), pp. 3894–3898, IEEE, Mar. 2017.
- [12] R. Shafipour, A. Khodabakhsh, G. Mateos, and E. Nikolova, "A Digraph Fourier Transform With Spread Frequency Components," May 2017. arXiv:1705.10821 [math].
- [13] S. Furutani, T. Shibahara, M. Akiyama, K. Hato, and M. Aida, "Graph Signal Processing for Directed Graphs Based on the Hermitian Laplacian," in *Machine Learning and Knowledge Discovery in Databases* (U. Brefeld, E. Fromont, A. Hotho, A. Knobbe, M. Maathuis, and C. R. Bardet, eds.), vol. 11906, pp. 447–463, Cham: Springer International Publishing, 2020. Series Title: Lecture Notes in Computer Science.
- [14] B. Seifert and M. Püschel, "Digraph Signal Processing with Generalized Boundary Conditions," *IEEE Transactions on Signal Processing*, vol. 69, pp. 1422–1437, 2021. arXiv:2005.09762 [cs, eess].
- [15] A. Venkitaraman, S. Chatterjee, and P. Händel, "On Hilbert transform, analytic signal, and modulation analysis for signals over graphs," *Signal Processing*, vol. 156, pp. 106–115, Mar. 2019.
- [16] Y. Li, Y. Qiao, A. Wigderson, Y. Wigderson, and C. Zhang, "Connections between graphs and matrix spaces," *Israel Journal of Mathematics*, vol. 256, pp. 513–580, Sept. 2023.
- [17] J. Domingos and J. M. F. Moura, "Graph Fourier Transform: A Stable Approximation," *IEEE Transactions on Signal Processing*, vol. 68, pp. 4422–4437, 2020. arXiv:2001.05042 [eess].
- [18] K. Itoh, "Analysis of the phase unwrapping algorithm," *Applied Optics*, vol. 21, p. 2470, July 1982.
- [19] M. Felsberg and G. Sommer, "The monogenic signal," *IEEE Transactions on Signal Processing*, vol. 49, pp. 3136–3144, Dec. 2001.
- [20] M. Unser, K. Balac, and D. V. D. Ville, "The monogenic Riesz-Laplace wavelet transform," 2008.
- [21] R. Singh, A. Chakraborty, and B. S. Manoj, "Graph Fourier transform based on directed Laplacian," in *2016 International Conference on Signal Processing and Communications (SPCOM)*, (Bangalore, India), pp. 1–5, IEEE, June 2016.